

Dalton Transactions

Accepted Manuscript



This is an *Accepted Manuscript*, which has been through the Royal Society of Chemistry peer review process and has been accepted for publication.

Accepted Manuscripts are published online shortly after acceptance, before technical editing, formatting and proof reading. Using this free service, authors can make their results available to the community, in citable form, before we publish the edited article. We will replace this *Accepted Manuscript* with the edited and formatted *Advance Article* as soon as it is available.

You can find more information about *Accepted Manuscripts* in the [Information for Authors](#).

Please note that technical editing may introduce minor changes to the text and/or graphics, which may alter content. The journal's standard [Terms & Conditions](#) and the [Ethical guidelines](#) still apply. In no event shall the Royal Society of Chemistry be held responsible for any errors or omissions in this *Accepted Manuscript* or any consequences arising from the use of any information it contains.

Cite this: DOI: 10.1039/c0xx00000x

www.rsc.org/dalton

COMMUNICATION

A novel manganese-doped large polyoxotitanate nanocluster

Yang Chen,^{*,a} Elzbieta Trzop,^a Anna Makal,^{a,b} Yu-Sheng Chen^c and Philip Coppens^{*,a}

Received (in XXX, XXX) XthXXXXXXXXXX 20XX, Accepted Xth XXXXXXXXXXXX 20XX

DOI: 10.1039/b000000x

A large manganese-doped polyoxotitanate nanocluster $\text{Ti}_{28}\text{MnO}_{38}(\text{OEt})_{40}\text{H}_2$, has been synthesized solvothermally. Its structure is arranged around the four-coordinate Mn^{2+} dopant atom in a Keggin-type structure. A significant reduction of the band gap relative to that of undoped polyoxotitanate clusters is observed.

Polyoxotitanate nanoparticles play a crucial role as anodes in photovoltaic cells,¹ and as photocatalysts in processes such as the oxidation of organic compounds in polluted air and wastewater.² However, pure TiO_2 does not absorb in the visible light region. Anatase, for example, has an indirect band gap of 3.21 eV.³ Considerable experimental and theoretical attention has therefore been directed to reduction of the band gap by doping of TiO_2 .⁴⁻⁹ Asai *et al.* reported ab-initio calculations on a supercell of rutile doped with the 3d transition metals V, Cr, Mn, Fe, Co and Ni.¹⁰ They found significant variations in the band gap due to insertion of dopant energy levels in the gap of the semiconductor, especially for Mn and Cr dopants.

However, little experimental information on the structure of doped nanoparticles has been available until recently, when we and others have synthesized and crystallized a series of polyoxotitanate nanoclusters and analysed their structure and those of chromophore-sensitized derivatives by crystallographic methods.¹¹⁻¹⁶ We report here the structure and band gap of a large doped polyoxotitanate cluster in which the Mn dopant is located in a central position in the nanoparticle.

Solvothermal reaction of titanium(IV) ethoxide with manganese(III) acetate dihydrate in the presence of ammonium bromide in ethanol at 150 °C for 66 hours generated the pale-yellow plate-shaped crystals of $\text{Ti}_{28}\text{MnO}_{38}(\text{OEt})_{40}\text{H}_2 \cdot \text{EtOH}$. Without the addition of ammonium bromide to adjust the pH of the reaction mixture the title compound was not formed. The valency of +2 of the manganese dopant was confirmed by X-ray absorption spectroscopy (Fig. S1, ESI†). Nevertheless, replacing manganese(III) acetate by manganese(II) acetate as starting material did not produce the title compound. The EDS (energy-dispersive X-ray spectroscopy) spectrum of $\text{Ti}_{28}\text{MnO}_{38}(\text{OEt})_{40}\text{H}_2 \cdot \text{EtOH}$ showed atomic ratio of Ti to Mn of 27.11 : 1 (Fig. S2, ESI†), which is close to the 28 : 1 value derived from the crystal structure.

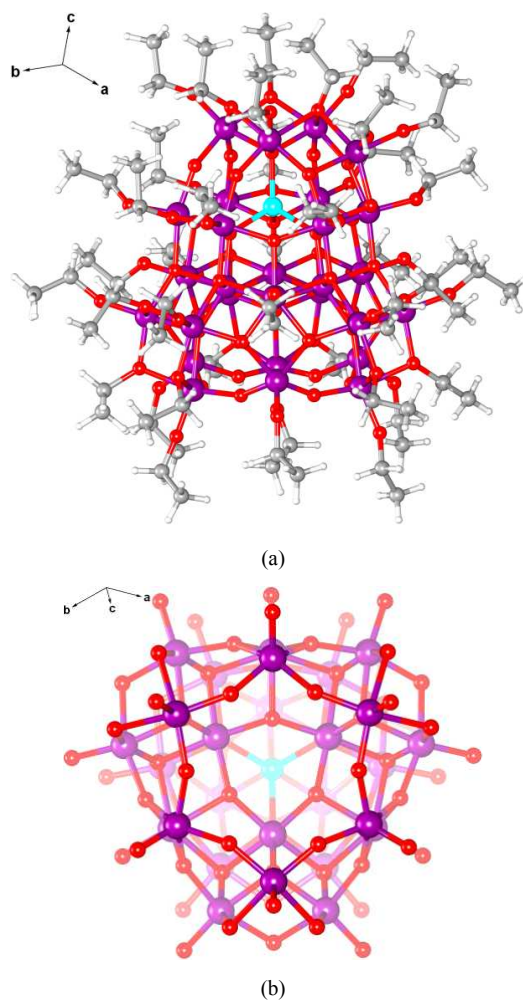


Fig. 1 (a) The molecular structure of $\text{Ti}_{28}\text{MnO}_{38}(\text{OEt})_{40}\text{H}_2$. Ti, purple; Mn, cyan; O, red; C, grey; H, light grey. For clarity only the major components of the disordered ethyl groups and of the triply-disordered Ti are shown (see Fig. S3 for details). (b) Perspective view of the TiO core of the cluster looking down along its longitudinal direction. Ethyl groups of the ethoxy ligands have been omitted for clarity.

Crystallographic studies reveal the structure shown in Fig. 1. The asymmetric unit of the triclinic space group $P\bar{1}$ (Table S1) contains one TiO cluster and one ethanol solvent molecule.

Charge neutrality requires the presence of two hydrogen atoms attached to peripheral core oxygen atoms, but these hydrogen atoms could not be located in the difference maps. The same difficulty was encountered by Lv *et al.* in the structure determination of $[\text{Ti}_{28}\text{O}_{38}(\text{OEt})_{40}\text{H}_2\text{LnCl}]$.¹¹ A similar protonation has been observed in $[\text{Ti}_{18}\text{O}_{28}\text{H}(\text{O}^i\text{Bu})]$.¹⁷ As shown in Fig. 1b, the TiO core of $\text{Ti}_{28}\text{MnO}_{38}(\text{OEt})_{40}\text{H}_2$ exhibits an approximate C_{3v} symmetry when viewed along its long direction. The EtOH molecule is located at the bottom of the cluster adjacent to the Ti_6O_6 -crown. Unlike previously described doped Ti_{28} clusters¹¹ in the current case the core is built around the centrally located four-coordinated Mn(II) atom in a Keggin-type arrangement.¹⁸ The cluster contains three six-coordinated Ti atoms in its inner layer, and three five-coordinated Ti atoms, three seven-coordinated Ti atoms and eighteen six-coordinated Ti atoms in its outer layer (Fig. 2). The Ti1 atom is disordered over three positions with occupancies of 80 % (Ti1), 15 % (Ti1A) and 5 % (Ti1B), respectively (Fig. S3, ESI†). The average Mn-O bond length is longer than the corresponding Ti-O bond lengths in Ti_{28}Ln (Ln = La, Ce),¹¹ $\text{Ti}_{28.5}\text{AO}_{38}(\text{OEt})_{39}$ (A = Li, Na),¹⁹ and $\text{Ti}_{17}\text{O}_{24}(\text{O}^i\text{Pr})_{20}$,²⁰ but shorter than the Mn-O bond in $\text{Ti}_{14}\text{MnO}_{14}(\text{OEt})_{28}\text{H}_2$ ²¹ (Table S2).

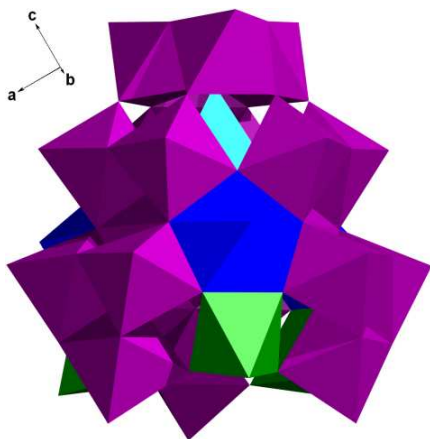


Fig. 2 Polyhedral representation of the manganese and titanium atoms in the metal oxide core, shaded according to coordination number: four-coordinate (cyan, Mn), five- (green, Ti), six- (purple, Ti), seven- (blue, Ti).

It is noteworthy that the upper part of $\text{Ti}_{28}\text{MnO}_{38}(\text{OEt})_{40}\text{H}_2$ has the same connectivity as $\text{Ti}_{17}\text{O}_{24}(\text{O}^i\text{Pr})_{20}$ (Fig. S4, ESI†),²⁰ while the bottom part forms a TiO-nanocage, as illustrated in Fig. 3. Unlike $\text{Ti}_{28}\text{LnO}_{36}(\text{OH})_2(\text{OEt})_{40}\text{Cl}$ (Ln = La, Ce),¹¹ and $\text{Ti}_{28.5}\text{AO}_{38}(\text{OEt})_{39}$ (A = Li, Na),¹⁹ in which dopant is located at the bottom of the nanocages, the cage in $\text{Ti}_{28}\text{MnO}_{38}(\text{OEt})_{40}\text{H}_2$ is open, with a cross section of 5.439\AA (average of three O...O distances, see Fig. S5(ESI†)). This is larger than corresponding values in $\text{Ti}_{28}\text{LnO}_{36}(\text{OH})_2(\text{OEt})_{40}\text{Cl}$,¹¹ and $\text{Ti}_{28.5}\text{AO}_{38}(\text{OEt})_{39}$ (Table 1),¹⁹ indicating that the opening of the nanocage is flexible and its size is sensitive to the nature and location of the metal dopants. A related non-doped Nb_{27} cluster with a similar architecture has been reported.²²

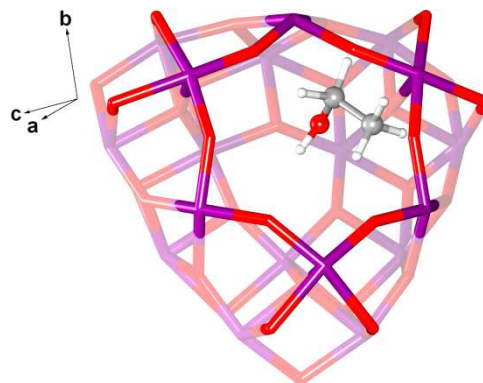


Fig. 3 Perspective view of the Ti/O-based nanocage in the $\text{Ti}_{28}\text{MnO}_{38}(\text{OEt})_{40}\text{H}_2$ cluster as well as the ethanol guest molecule located at the outside of the hexagon.

Table 1 Opening sizes of the nanocages in different metal-doped polyoxotitanate clusters.

Polyoxotitanate nanocluster	Three O...O distances of nanocage (Å)	Average of three O...O distances of nanocage (Å)
$\text{Ti}_{28}\text{MnO}_{38}(\text{OEt})_{40}\text{H}_2$	5.417(6)	5.439(6)
	5.441(6)	
	5.460(6)	
$\text{Ti}_{28.5}\text{LiO}_{38}(\text{OEt})_{39}$ ¹⁹	5.248(5)	5.383(6)
	5.248(6)	
	5.652(6)	
$\text{Ti}_{28.5}\text{NaO}_{38}(\text{OEt})_{39}$ ¹⁹	5.130(6)	5.338(6)
	5.352(6)	
	5.530(6)	
$\text{Ti}_{28}\text{LaO}_{36}(\text{OH})_2(\text{OEt})_{40}\text{Cl}$ ¹¹	5.077	5.095
	5.083	
	5.124	
$\text{Ti}_{28}\text{CeO}_{36}(\text{OH})_2(\text{OEt})_{40}\text{Cl}$ ¹¹	5.043	5.068
	5.054	
	5.106	

The diffuse-reflectance spectrum of the crystalline solid was measured at room temperature and processed with the Kubelka-Munkfunction²³ to give a band gap of 2.74 eV (Fig. 4). The band gap is thus significantly red-shifted compared with those of an undoped Ti_{28} cluster (indirect band gap 3.43 eV),²⁴ or the one measured with reflectance spectroscopy for commercial anatase (3.19 eV).²¹ The value is comparable to that of $\text{Ti}_{14}\text{MnO}_{16}(\text{OEt})_{28}\text{H}_2$ (2.64 eV).²¹ The difference between the two results for the two Mn-doped clusters is small and may not be significant.²⁵ To eliminate the possibility of sample decomposition, its powder pattern was recorded after the measurement of the reflectance spectrum. It was found to correspond to the pattern constructed from the known structure and cell dimensions of the title compound and to be very different from that of anatase or Mn-doped anatase (see Figs. S7 and S8).

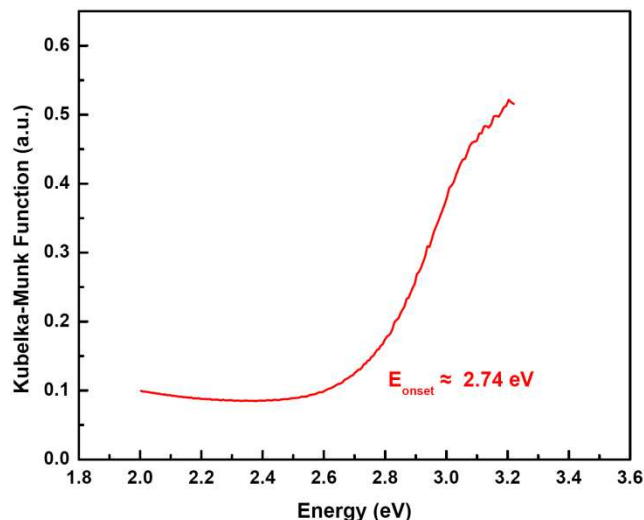


Fig. 4 Solid state optical diffuse-reflectance spectrum of $\text{Ti}_{28}\text{MnO}_{38}(\text{OEt})_{40}\text{H}_2\cdot\text{EtOH}$ derived from diffuse reflectance data at room temperature.

In summary, the manganese dopant in $\text{Ti}_{28}\text{MnO}_{38}(\text{OEt})_{40}\text{H}_2$ adopts a tetrahedral coordination geometry at a central location in the cluster, similar to that in the smaller cluster $\text{Ti}_{14}\text{MnO}_{16}(\text{OEt})_{28}\text{H}_2$, but unlike the dopant position in previously described Ti_{28} clusters. The band gap is red-shifted compared with undoped polyoxotitanate nanoclusters and anatase, leading to desired absorption in the visible region. In addition, the nanocage at the lower part of the cluster is not terminated by a dopant atom although an ethanol molecule is located just below the cage with its OH^- group pointing toward the center of Ti_6O_6 -crown.

We thank Peter J. Bush, Director of the South Campus Instrument Center, University at Buffalo, for assistance with the EDS spectrum analysis. This work was funded by the Division of Chemical Sciences, Geosciences, and Biosciences, Office of Basic Energy Sciences of the U.S. Department of Energy through Grant DE-FG02-02ER15372. ChemMatCars is principally supported by the National Science Foundation/Department of Energy under Grant CHE-0822838. Use of the APS was supported by the U.S. Department of Energy, Office of Science, Office of Basic Energy Sciences, under Contract DE-AC02-06CH11357.

Notes and references

^aChemistry Department, University at Buffalo, SUNY, Buffalo, New York 14260-3000, United States

^bDepartment of Chemistry, University of Warsaw, Pasteura 1, 02-093 Warszawa, Poland

^cChemMat CARS, University of Chicago, Chicago, Illinois 60637, United States

*Fax: 1-716-645-6948; Tel: 1-716-645-4273; E-mail:

coppens@buffalo.edu, ychen37@buffalo.edu

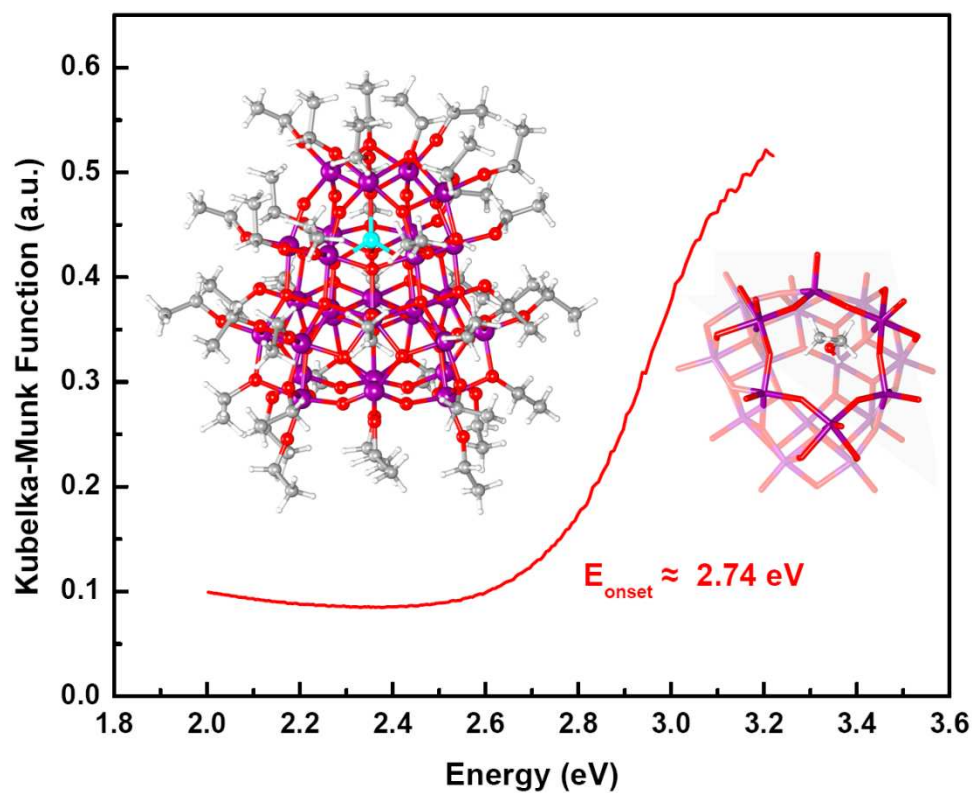
†Electronic Supplementary Information (ESI) available: CCDC 970095. For crystallographic data in CIF or other electronic format, synthesis, Tables S1 and S2, Figs. S1-S6. See DOI: 10.1039/b000000x/

‡ XANES spectra at the Mn absorption edge were collected at beamline 15-ID at the Advanced Photon Source (APS). SEM/EDS micro-analysis was performed on a Hitachi SU70 FESEM operating at 20keV. The solid state optical diffuse-reflection experiments were performed on a Perkin-

Elmer Lambda 35 UV-Vis spectrometer equipped with an integrating sphere for diffuse reflectance spectroscopy.

1. M. Gratzel, *Acc. Chem. Res.*, 2009, **42**, 1788-1798.
2. A. L. Linsebigler, G. Lu and J. T. Yates, *Chem. Rev.*, 1995, **95**, 735-758.
3. N. Serpone and D. L. a. R. Khairutdinov, *J. Phys. Chem.*, 1995, **99**, 16646-16654.
4. A. Zaleska, *Recent Patents on Engineering*, 2008, **2**, 157-164.
5. Y. H. Zhang, F. Z. Lv, T. Wu, L. Yu, R. Zhang, B. Shen, X. H. Meng, Z. F. Ye and P. K. Chu, *J. Sol-Gel Sci. Technol.*, 2011, **59**, 387-391.
6. F. Spadavecchia, G. Cappelletti, S. Ardizzone, M. Ceotto and L. Falciola, *J. Phys. Chem. C*, 2011, **115**, 6381-6391.
7. S. In, A. Orlov, R. Berg, F. Garcia, S. Pedrosa-Jimenez, M. S. Tikhov, D. S. Wright and R. M. Lambert, *J. Am. Chem. Soc.*, 2007, **129**, 13790-+.
8. M. H. Zhou, J. G. Yu and B. Cheng, *J. Hazard. Mater.*, 2006, **137**, 1838-1847.
9. M. Iwasaki, M. Hara, H. Kawada, H. Tada and S. Ito, *Journal of Colloid and Interface Science*, 2000, **224**, 202-204.
10. T. Umabayashi, T. Yamaki, H. Itoh and K. Asai, *J. Phys. Chem. Solids*, 2002, **63**, 1909-1920.
11. Y. Lv, J. Willkomm, M. Leskes, A. Steiner, T. C. King, L. Gan, E. Reisner, P. T. Wood and D. S. Wright, *Chem. Eur. J.*, 2012, **18**, 11867-11870.
12. S. Eslava, B. P. R. Goodwill, M. McPartlin and D. S. Wright, *Inorg. Chem.*, 2011, **50**, 5655-5662.
13. S. In, A. Orlov, F. Garcia, M. Tikhov, D. S. Wright and R. M. Lambert, *Chem. Commun.*, 2006, 4236-4238.
14. L. Rozes and C. Sanchez, *Chem. Soc. Rev.*, 2011, **40**, 1006-1030.
15. J. D. Sokolow, E. Trzop, Y. Chen, J. Tang, L. J. Allen, R. H. Crabtree, J. B. Benedict and P. Coppens, *J. Am. Chem. Soc.*, 2012, **134**, 11695-11700.
16. J. B. Benedict and P. Coppens, *J. Am. Chem. Soc.*, 2010, **132**, 2938-2944.
17. C. F. Campana, Y. Chen, V. W. Day, W. G. Klemperer and R. A. Sparks, *J. Chem. Soc., Dalton Trans.*, 1996, 691-702.
18. J. F. Keggin, *Proc. R. Soc. A*, 1934, **144**, 75-100.
19. Y. Chen, E. Trzop, A. Makal, J. D. Sokolow and P. Coppens, *Inorg. Chem.*, 2013, **52**, 4750-4752.
20. N. Steunou, G. Kickelbick, K. Boubekeur and C. M. Sanchez, *J. Chem. Soc.-Dalton Trans.*, 1999, 3653-3655.
21. Y. Chen, J. Sokolow, E. Trzop, Y.-S. Chen and P. Coppens, *J. Chin. Chem. Soc.*, 2013, **60**, 887-890.
22. R. Tsunashima, D.-L. Long, H. Miras, N. D. Gabb, C. Pradeep and L. Cronin, *Angew. Chemie-Int. Ed.*, 2010, **49**, 113-116.
23. W. W. Wendlandt and H. G. Hecht, *Reflectance spectroscopy*, Interscience Publishers, New York, 1966.
24. J. B. Benedict, R. Freindorf, E. Trzop, J. Cogswell and P. Coppens, *J. Am. Chem. Soc.*, 2010, **132**, 13669-13671.
25. A. B. Murphy, *Sol. Energy Mater. Sol. Cells*, 2007, **91**, 1326-1337.

Table of Contents:



The largest manganese-doped polyoxotitanate nanocluster so far, $\text{Ti}_{28}\text{MnO}_{36}(\text{OH})_2(\text{OEt})_{40}$, is reported. The coordination of the manganese dopant in polyoxotitanate nanoclusters and the impact of manganese doping on the band gap of the clusters is discussed.